Pergamon

www.elsevier.com/locate/jappmathmech

PII: S0021-8928(03)00148-5

J. Appl. Maths Mechs, Vol. 67, No. 6, pp. 921–935, 2003

0021-8928/$—see front matter

IMPLICIT ALGORITHMS FOR SOLVING THE CAUCHY PROBLEM FOR THE EQUATIONS OF THE DYNAMICS OF MECHANICAL SYSTEMS†

A. N. DANILIN, Ye. B. KUZNETSOV and V. I. SHALASHILIN

Moscow

e-mail: ad@essp.ru; kuznetsov@mai.ru; nadya@lanit.ru

(*Received* 23 *December* 2002)

It is shown that in the numerical solution of the Cauchy problem for systems of second-order ordinary differential equations, when solved for the highest-order derivative, it is possible to construct simple and economical implicit computational algorithms for step-by-step integration without using laborious iterative procedures based on processes of the Newton–Raphson iterative type. The initial problem must first be transformed to a new argument – the length of its integral curve. Such a transformation is carried out using an equation relating the initial parameter of the problem to the length of the integral curve. The linear acceleration method is used as an example to demonstrate the procedure of constructing an implicit algorithm using simple iterations for the numerical solution of the transformed Cauchy problem. Propositions concerning the computational properties of the iterative process are formulated and proved. Explicit estimates are given for an integration stepsize that guarantees the convergence of the simple iterations. The efficacy of the proposed procedure is demonstrated by the numerical solution of three problems. A comparative analysis is carried out of the numerical solutions obtained with and without parametrization of the initial problems in these three settings. As a qualitative test the problem of the celestial mechanics of the "Pleiades" is considered. The second example is devoted to modelling the non-linear dynamics of an elastic flexible rod fixed at one end as a cantilever and coiled in its initial (static) state into a ring by a bending moment. The third example demonstrates the numerical solution of the problem of the "unfolding" of a mechanical system consisting of three flexible rods with given control input.

1. FORMULATION OF THE PROBLEM

We will consider the Cauchy problem for a system of second-order ordinary differential equations solved for the highest order derivative:

$$\ddot{u} = f(t, u, \dot{u}), \quad u(t_0) = u_0, \quad \dot{u}(t_0) = v_0 \tag{1.1}$$

where $u(t)$ is an unknown vector function describing the displacement of a point in Euclidean n-space, and the vector function $f = f(t, u, v)$, acting as an operator $f: \mathbb{R}^{2n+1} \to \mathbb{R}^n$, is the acceleration of the point in the space $\mathbb{R}^n$, depending on the time $t \in \mathbb{R}$, the displacement and the velocity $v = \dot{u}$.

The mathematical modelling of many physical phenomena reduces to the system of equations (1.1). In particular, applied problems associated with the modelling of dynamical processes in structures and continuous media lead to Eqs (1.1) (see, e.g, [1–6]).

We will assume that $f \in \mathbb{C}^2(D)$, where $D \subset \mathbb{R}^{2n+1}$ is some domain in Euclidean space $\mathbb{R}^{2n+1}$. Then, as is well known [7, 8], the Cauchy problem has a unique solution in D for given initial data $y_0 = [u_0, v_0, t_0]^T \in D$. Thus, under the conditions just formulated, through any point of the domain D there passes a unique smooth integral curve (IC) $y(t) = [u(t), v(t), t]^T$ that satisfies the system of equations (1.1), and the solution of problem (1.1) reduces to constructing an IC in the domain D passing through the point x_0.

We will denote the scalar product of the functions f and g and the norm of a function f in some Euclidean space by fg and $\|f\| = \sqrt{ff}$, respectively.

The purpose of this paper is to study the system of equations (1.1) from the position of method of parametric continuation of the solution [9] and to construct effective implicit computation schemes for solving it when a certain additional change of variables, called the best parametrization, is applied (see [10–15]).

†*Prikl. Mat. Mekh.* Vol. 67, No. 6, pp. 1051–1067, 2003.

2. PARAMETRIZATION OF THE EQUATIONS

Introducing in D a smooth real function $\lambda = \lambda(y) = \lambda(u, \upsilon, t) \in \mathbb{C}^3(D)$, let us replace the independent variable t by the parameter λ. When that is done, the differential characteristic J of the function λ – namely, its total derivative with respect to time along an IC: $J(y) = J(u, \upsilon, t) = \dot{\lambda}[y(t)]$ – is of major importance. We shall assume that $J(y) \neq 0$ in D. Then the parameter function may be represented in terms of its differential characteristic as a definite integral along some IC:

$$\lambda(y) = \lambda_0 + \int_{t_0}^{t} J[y(t)]dt$$

By changing to the parameter λ we can convert the system of differential equations (1.1) into an autonomous first-order system in the phase space $\mathbb{R}^{2n+1}$

$$y' = F(y), \quad y(\lambda_0) = y_0, \quad F = J^{-1}[\upsilon, f, 1]^T \in \mathbb{C}^2(D) \tag{2.1}$$

where the prime denotes the total derivative with respect to λ.

The function J has the meaning of a differential normalizing factor in the transformation from the time t to the parameter λ. In particular, if $J \equiv 1$, then $\lambda = t + (\lambda_0 - t_0)$. Through parametrization one can improve the metric properties of the right-hand side of Eq. (2.1). It has been shown [9–14] that the optimum improvement (i.e. the best parametrization) is achieved when λ is taken to be the length of an IC in the Euclidean space $\mathbb{R}^{2n+1}$. Corresponding to this choice is the following equation in differential form

$$d\lambda^2 = dt^2 + dudu + d\upsilon d\upsilon \tag{2.2}$$

or the equation for the normalizing factor

$$J(y) = \sqrt{1 + \upsilon\upsilon + f(y)f(y)} \tag{2.3}$$

Obviously,

$$J^{-1}(y) = t'$$

It follows from formulae (2.1)–(2.3) that in the best parametrization the norm of the right-hand side of Eq. (2.1) has an important property: it equals unity in the domain D. The change to the argument λ also ensures the best conditionality for the linearized systems of equations obtained when implementing step-by-step procedures for the numerical constructing of ICs in problem (1.1) by parametric continuation, and in this sense the change to λ has been called the best parametrization and λ itself the best parameter.

3. THE NUMERICAL SCHEME FOR SOLVING THE CAUCHY PROBLEM

Problem (1.1) or (2.1) can be solved by using various approximate numerical integration schemes for systems of differential equations [16–18], such as the Runge–Kutta, Adams–Moulton, Milne, etc. methods. Special mention should be made among these of methods of second- and third-order precision, which lead as a rule to implicit integration schemes, such as the method of central differences, and the Houbolt, Newmark and Wilson methods [2–4]. Much use has been made in the practical solution of dynamics problems of Wilsons method, which is a certain modification of the linear acceleration method, in which, when integrating Eq. (1.1), one replaces the acceleration $\ddot{u}$ by piecewise-linear function over a small interval of time (the integration stepsize). Consequently, the velocity $\upsilon = \dot{u}$ and the displacement u itself are approximated by second- and third-order splines, respectively.

We shall consider a generalization of the linear acceleration method to the system of equations (2.1) with the best parametrization [15, 19]. To that end, we will represent the unknown vector t as $y = [u, x]^T$, where $x = [\upsilon, t]^T \in \mathbb{R}^{n+1}$, that is, we single out from y a vector x which uniquely defines the acceleration $\ddot{u} = J\upsilon'$. Accordingly, the right-hand side of Eq. (2.1) will be written as $F = J^{-1}[\upsilon, g]^T$, where $g = [f, 1]^T$.

Relations (2.2) and (2.3) imply the equality $J^{-2} + u'u' + \upsilon'\upsilon' = 1$, whence, in view of the formula $\upsilon' = J^{-1}f$, we obtain $J^{-1} = \sqrt{1 - u'u'}/\sqrt{1 + ff}$. With this expression, system (2.1) can be rewritten as a system of differential equations

$$u' = J^{-1}\upsilon \tag{3.1}$$

$$x' = J^{-1}g = \sqrt{1 - u'u'}\,e(u, x) \tag{3.2}$$

where $e(u, x) = g/\sqrt{1 + ff} = g/\|g\|$ is a unit vector in the space $\mathbb{R}^{n+1}$, collinear with the vector g. In what follows we shall use the first equality of (3.2) in the form

$$x' = \hat{g} \tag{3.3}$$

where $\hat{g} = J^{-1}g = [\hat{f}, J^{-1}]^T, \hat{f} = J^{-1}f$.

We will divide the domain of variation of the integration parameter λ into intervals by points $\lambda_0 < \lambda_1 < \ldots < \lambda_n < \ldots$ and approximate the variable x' (in parametrized form) in each interval $\lambda \in (\lambda_n, \lambda_{n+1})$ by a linear function

$$x'(\lambda) = x'_n + \frac{\tau}{\Delta\lambda_n}(x'_{n+1} - x'_n) \tag{3.4}$$

where $\tau = \lambda - \lambda_n$ $\Delta\lambda_n = \lambda_{n+1} - \lambda_n$.

We now integrate equality (3.4) with respect to the parameter τ. Taking the representation $x = [\upsilon, t]^T$ into account, we obtain

$$\upsilon(\lambda_n + \tau) = \upsilon_n + \tau\upsilon'_n + \frac{\tau^2}{2\Delta\lambda_n}(\upsilon'_{n+1} - \upsilon'_n) \tag{3.5}$$

$$t(\lambda_n + \tau) = t_n + \tau t'_n + \frac{\tau^2}{2\Delta\lambda_n}(t'_{n+1} - t'_n) \tag{3.6}$$

To determine the function $u(\lambda_n + \tau)$, we use Eq. (3.1). Replacing J^{-1} by a linear approximation on the basis of formula (3.4) and using equality (3.5), we obtain an approximation of third-order precision for $u'(\lambda)$

$$u'(\lambda_n + \tau) = t'(\lambda_n + \tau)\upsilon(\lambda_n + \tau) = J_n^{-1}\upsilon_n + \tau\left[J_n^{-1}\upsilon'_n + \frac{1}{\Delta\lambda_n}(J_{n+1}^{-1} - J_n^{-1})\upsilon_n\right] +$$

$$+ \frac{\tau^2}{\Delta\lambda_n}\left[\frac{J_n^{-1}}{2}(\upsilon'_{n+1} - \upsilon'_n) + (J_{n+1}^{-1} - J_n^{-1})\upsilon'_n\right] + \frac{\tau^3}{2\Delta\lambda_n^2}(J_{n+1}^{-1} - J_n^{-1})(\upsilon'_{n+1} - \upsilon'_n)$$

Hence, integrating with respect to τ, we get an approximation for $u(\lambda)$ also

$$u(\lambda_n + \tau) = u_n + \tau J_n^{-1}\upsilon_n + \frac{\tau^2}{2}\left[J_n^{-1}\upsilon'_n + \frac{1}{\Delta\lambda_n}(J_{n+1}^{-1} - J_n^{-1})\upsilon_n\right] +$$

$$+ \frac{\tau^3}{3\Delta\lambda_n}\left[\frac{J_n^{-1}}{2}(\upsilon'_{n+1} - \upsilon'_n) + (J_{n+1}^{-1} - J_n^{-1})\upsilon'_n\right] + \frac{\tau^4}{8\Delta\lambda_n^2}(J_{n+1}^{-1} - J_n^{-1})(\upsilon'_{n+1} - \upsilon'_n) \tag{3.7}$$

Setting $\tau = \Delta\lambda_n$ in expressions (3.5)–(3.7), we obtain the following implicit numerical scheme for determining the quantities $u_{n+1} = u(\lambda_{n+1})$ and $x_{n+1} = x(\lambda_{n+1})$

$$u_{n+1} = u_n + \frac{\Delta\lambda_n}{2}(J_{n+1}^{-1} - J_n^{-1})\upsilon_n + \frac{(\Delta\lambda_n)^2}{24}[(3J_{n+1}^{-1} + J_n^{-1})\hat{f}_{n+1} + (5J_{n+1}^{-1} + 3J_n^{-1})\hat{f}_n] \tag{3.8}$$

$$x_{n+1} = x_n + \frac{\Delta\lambda_n}{2}(\hat{g}_{n+1} + \hat{g}_n) \tag{3.9}$$

where $\hat{f}_n = \hat{f}(u_n, x_n)$, and the initial data u_0 and $x_0 = [\upsilon_0, t_0]^T$ are known.

The numerical scheme (3.8), (3.9) has second-order precision for the vector $x = [\upsilon, t]^T$ and the displacement vector u, since the unknown vector x was approximated by a second-order spline and the displacement by a piecewise-smooth polynomial of the fourth order with continuous derivatives.

4. THE ITERATIVE PROCESS

The numerical scheme (3.8), (3.9) just obtained is implicit with respect to the unknown $y_{n+1} = [u_{n+1}, x_{n+1}]^T \in \mathbb{R}^{2n+1}$, and therefore, at each step, it is required to solve a system of $2n + 1$ non-linear equations. This solution may be treated from the viewpoint of the theory of smooth mappings [8] of the Euclidean space $\mathbb{R}^{2n+1}$, since it is a fixed point for a certain smooth diffeomorphic mapping, defined by the iterative scheme (3.8), (3.9) and acting on a compact subset of $\mathbb{R}^{2n+1}$. To demonstrate this, we will rewrite the scheme (3.8), (3.9) in the form

$$y = \Phi(y), \quad \Phi(y) = y_{n+1/2} + \Delta\lambda_n \Psi(y) \tag{4.1}$$

The solution of problem (4.1) is the unknown y_{n+1}, while the intermediate value $y_{n+1/2}$ and the function $\Psi(y)$ are determined from the data of the previous step by the respective formulae

$$y_{n+1/2} = \begin{bmatrix} u_n + \dfrac{\Delta\lambda_n}{2} J_n^{-1} \upsilon_n + \dfrac{(\Delta\lambda_n)^2}{8} J_n^{-1} \hat{f}_n \\ x_n + \dfrac{\Delta\lambda_n}{2} \bar{g}_n \end{bmatrix}, \quad \Psi(y) = \frac{1}{2} \begin{bmatrix} J^{-1}(y)\upsilon_n + \Delta\lambda_n H_n(y) \\ g(y) \end{bmatrix} \tag{4.2}$$

$$H_n(y) = \frac{1}{12}\{[3J^{-1}(y) + J_n^{-1}]\hat{f}(y) + 5J^{-1}(y)\hat{f}_n\}$$

Then the solution of the non-linear equation (4.1) is equivalent to determining the fixed points of the mapping

$$\tilde{y} = \Phi(y), \quad \Phi \in \mathbb{C}^2(D) \tag{4.3}$$

defined in the space $\mathbb{R}^{2n+1}$.

Lemma. For system (2.1), (2.2) with the best parametrization, the mapping (4.3) is defined in a bi-sphere $B_{r,A}(y_{n+1/2})$ with centre at the point $y_{n+1/2} = [u_{n+1/2}, x_{n+1/2}]^T$, where

$$B_{r,A}(y_{n+1/2}) = \{y = [u, x]^T : \|u - u_{n+1/2}\| \le A, \|x - x_{n+1/2}\| \le r\} \tag{4.4}$$

$$r = r(\Delta\lambda_n) = \frac{\Delta\lambda_n}{2}, \quad A = A(\upsilon_n, \Delta\lambda_n) = \frac{\Delta\lambda_n}{2}\left(\|\upsilon_n\| + \frac{3}{4}\Delta\lambda_n\right) \tag{4.5}$$

Proof. Let us estimate the norms of the components of the vector function $\Psi(y)$ responsible for the norms $\|u - u_{n+1/2}\|$ and $\|x - x_{n+1/2}\|$, respectively. Evaluating the square of the norm of the first component, we have

$$\left\|J^{-1}(y)\upsilon_n + \Delta\lambda_n H_n(y)\right\|^2 = J^{-2}(y)\|\upsilon_n\|^2 + 2\Delta\lambda_n J^{-1}(y)\upsilon_n H_n(y) + (\Delta\lambda_n)^2\|H_n(y)\|^2$$

It follows from expression (2.3) that

$$J^{-1}(y) = \frac{1}{\sqrt{1 + \upsilon\upsilon + f(y)f(y)}} \le 1$$

for any values of y. Using the last inequality and the triangle inequality, we obtain

$$\left\|J^{-1}(y)\upsilon_n + \Delta\lambda_n H_n(y)\right\|^2 \le \|\upsilon_n\|^2 + \frac{2\Delta\lambda_n}{3}\upsilon_n\left(\hat{f} + \frac{5}{4}\hat{f}_n\right) + \frac{(\Delta\lambda_n)^2}{9}\left\|\hat{f} + \frac{5}{4}\hat{f}_n\right\|^2 =$$

$$= \left\|\upsilon_n + \frac{\Delta\lambda_n}{3}\left(\hat{f} + \frac{5}{4}\hat{f}_n\right)\right\|^2 \le \left(\|\upsilon_n\| + \frac{\Delta\lambda_n}{3}\left\|\hat{f} + \frac{5}{4}\hat{f}_n\right\|\right)^2$$

Since

$$\hat{f} = \frac{f}{\sqrt{1 + vv + f(y)f(y)}} \leq 1$$

it follows that

$$\left\| \hat{f} + \frac{5}{4}\hat{f}_n \right\| \leq \frac{9}{4}$$

Therefore

$$\left\| J^{-1}(y)v_n + \Delta\lambda_n H_n(y) \right\| \leq \|v_n\| + \frac{3}{4}\Delta\lambda_n$$

This enables us, with relation (4.1) and (4.2), to give an estimate

$$\|u - u_{n+1/2}\| \leq \frac{\Delta\lambda_n}{2}\left(\|v_n\| + \frac{3}{4}\Delta\lambda_n \right)$$

Using the estimate

$$\|\hat{g}\| \leq 1, \quad \hat{g} = J^{-1}g = \frac{g}{\sqrt{vv + g(y)g(y)}}$$

for the second component of the vector function $\Psi(y)$, we obtain an estimate for the norm $\|x - x_{n+1/2}\|$ also:

$$\|x - x_{n+1/2}\| \leq \frac{\Delta\lambda_n}{2}$$

In sum, we obtain formulae (4.4) and (4.5), which proves the lemma.

Thus, the solution of non-linear equation (4.1) is equivalent to determining the fixed points of the twice continuously differentiable mapping $\tilde{y} = \Phi(y)$, which is defined on the compact set (4.4), (4.5).

Remark 1. The manifold (4.4), (4.5) is non-isotropic in the subspaces of the vectors x and u: the vector x satisfies an estimate which is not explicitly dependent on the preceeding point of the integration $y_n = [u_n, v_n, t_n]^T$; the estimate for the displacement vector u, however, depends explicitly on v_n. This reflects the fact that the difference scheme we have constructed does not give the velocity and the displacement equal treatment, which in turn results from the adaptation of the solution to the analytical characteristics of the IC being computed (which is in turn a corollary of the best parametrization). However, this property does not impede the construction of effective computational procedures.

In what follows, the contractive property of the mapping $\tilde{y} = \Phi(y)$ will be proved, and the condition under which this property holds will be formulated.

Theorem 1. A value of the quantity $\Delta\lambda_n$ always exists for which a solution of the non-linear equation (4.1) exists, is unique, and can be constructed using the iterative process

$$y^{k+1} = \Phi(y^k), \quad y^0 = y_{n+1/2} \tag{4.6}$$

as the limit

$$y_{n+1} = y = \lim y^k, \quad k \to \infty$$

Proof. Consider the mapping (4.3), for which, by the lemma, $y \in B_{r,A}(y_{n+1/2})$. Let us estimate the difference quotient

$$\omega(\Phi; y_1, y_2) = \frac{\|\tilde{y}_1 - \tilde{y}_2\|}{\|y_1 - y_2\|}$$

for two arbitrary vectors $y_1, y_2 \in B_{r,A}(y_{n+1/2})$. Using relations (4.1) and (4.2), as well as the inclusion $\Psi \in \mathbb{C}^2(B_{r,A}(y_{n+1/2}))$, we obtain $\omega(\Phi; y_1, y_2) \leq C$, where the constant C depends on v_n and $\Delta\lambda_n$ and has the form $C = \Delta\lambda_n M(v_n, \Delta\lambda_n)$, with $M(v_n, \Delta\lambda_n) \to \|\Psi'(y_n)\|$ as $\Delta\lambda_n \to 0$. Consequently, for sufficiently small $\Delta\lambda_n$, we have $C < 1$ and $\|\tilde{y}_1 - \tilde{y}_2\| \leq C\|y_1 - y_2\|$, that is, the mapping (4.3) is contractive in the bi-sphere $B_{r,A}(y_{n+1/2})$. This implies the statement of the theorem.

Note that, using relation (3.9), one can put formula (3.8) in a form in which u_{n+1} is expressed in terms of known values at the preceeding step and the values of the components of the vector $x = [\upsilon, \tau]^T$ at the current step. Indeed, it follows from (3.9) that

$$J_{n+1}^{-1} + J_n^{-1} = \frac{2}{\Delta\lambda_n}(t_{n+1} - t_n), \quad \hat{f}_{n+1} + \hat{f}_n = \frac{2}{\Delta\lambda_n}(\upsilon_{n+1} - \upsilon_n) \tag{4.7}$$

By substituting expressions (4.7) into formula (3.8) we can rewrite the latter as

$$u_{n+1} = u_n + \frac{1}{6}(t_{n+1} - t_n)(\upsilon_{n+1} + 5\upsilon_n) + \frac{\Delta\lambda_n}{6}[\hat{f}_n(t_{n+1} - t_n) + J_{n+1}^{-1}(\upsilon_{n+1} - \upsilon_n)] \tag{4.8}$$

Finally, using the expression

$$J_{n+1}^{-1} = \frac{2}{\Delta\lambda_n}(t_{n+1} - t_n) - J_n^{-1}$$

which follows from the first relation of (4.7), we arrive at the formula

$$u_{n+1} = u_n + \frac{1}{2}(t_{n+1} - t_n)(\upsilon_{n+1} + \upsilon_n) + \frac{\Delta\lambda_n}{6}[\hat{f}_n(t_{n+1} - t_n) - J_n^{-1}(\upsilon_{n+1} - \upsilon_n)] \tag{4.9}$$

In this connection, let us single out a vector $x \in \mathbb{R}^{n+1}$ and consider the corresponding projection of the iterative process (4.6) onto the subspace $\mathbb{R}^{n+1}$. To do this, in accordance with relations (4.1) and (4.6), we introduce the iteration function

$$\phi(u, x) = x_{n+1/2} + \frac{\Delta\lambda_n}{2}\hat{g}(u, x)$$

where the variable u is the parameter, and consider the iterative process in the subspace $\mathbb{R}^{n+1}$ (for fixed u)

$$x^{k+1} = \phi^k = \phi(u, x^k), \quad x_{n+1} = x = \lim_{k\to\infty} x^{k+1} = \lim_{k\to\infty} \phi^k, \quad x^0 = \bar{x}_n + \frac{\Delta\lambda_n}{2} g_n \tag{4.10}$$

The iterative process (4.10) obviously converges provided the mapping $\bar{x} = \phi(u, x)$, defined for any u in the space $B_r(x_{n+1/2})$, $r = \Delta\lambda_n/2$, is contractive, that is, provided that $\Delta\lambda_n < 2$, the estimate being uniform with respect to the parameter u.

Thus, Theorem 1 can be strengthened if the iterative process to find x_{n+1} and u_{n+1} is organized as follows: First determine the vector x^{k+1} by formula (4.10), and then compute the variable $u = u^{k+1}$ by the following formula, which follows from (4.9)

$$\begin{aligned} u^{k+1} &= u_k + \frac{1}{2}(t^{k+1} - t_n)(\upsilon^{k+1} + \upsilon_n) + \frac{\Delta\lambda_n}{6}[\hat{f}_n(t^{k+1} - t_n) - J_n^{-1}(\upsilon^{k+1} - \upsilon_n)] \\ u^0 &= u_n + \frac{\Delta\lambda_n}{2} J_n^{-1}\upsilon_n + \frac{(\Delta\lambda_n)^2}{8} J_n^{-1}\hat{f}_n \end{aligned} \tag{4.11}$$

In sum, we have proved the following theorem.

Theorem 2. A solution of non-linear equation (4.1) exists and is unique, provided that $\Delta\lambda_n < 2$; it can be constructed using the iterative process (4.10), (4.11).

Remark 2. The condition $\Delta\lambda_n < 2$, which ensures convergence of the iterative process (4.10), is sufficient but not necessary. In some problems the integration stepsize that guarantees convergence may considerably exceed unity. An example is the problem, considered below, of the free vibrations of a flexible rod.

Remark 3. An analogous contractive property for the vector $x = [\upsilon, t]^T$ may also be constructed for other methods for approximating the solution vector (the Newmark, Wilson, Houbolt, etc. methods [2]) which are widely used for the numerical integration of dynamic systems.

5. EXAMPLES

Three problems will be considered below. In all cases, the numerical results obtained with an without using the parametrization procedure will be compared. The effectiveness of the implicit integration scheme (4.11), (3.9) for the parametrized equations will be demonstrated compared with the integration of the initial (non-parametrized) equations by an implicit scheme of the linear acceleration method [3, 4]

$$u_{n+1} = u_n + \Delta t_n v_n + \frac{\Delta t_n^2}{6}(f_{n+1} + 2f_n), \quad v_{n+1} = v_n + \frac{\Delta t_n}{2}(f_{n+1} + f_n) \tag{5.1}$$

These formulae follow from relations (3.8), (3.9) or (4.11), (3.9) if we set $\Delta\lambda_n = \Delta t_n$ and $J_n^{-1} = 1$ for all values of n.

The "Pleiades" test problem was solved for several values of the integration stepsize, constant over some interval along the IC or the interval in which the initial argument of the problem varied.

For the second and third problems, the solution was implemented with automatic control of the length of the integration stepsize along an IC of the solution: The step was chosen subject to the condition that the local integration error, evaluated using Richardson extrapolation [16], should not exceed a prescribed value δ. For comparison with known solution procedures, both problems were integrated using an implicit linear acceleration scheme (5.1) without a parametrization procedure, but using Newton–Raphson iteration as well as a modified version of that method. The solution was similarly implemented with the length of the integration stepsize along the axis of the time parameter controlled by estimating the local integration error (otherwise the integration time turned out to be too long). The Jacobian was evaluated numerically, while the corresponding system of algebraic equations was solved by Cholesky's method. In the modified Newton–Raphson method, the Jacobian and the solution of the system of algebraic equations were computed for each 10 steps of the time parameter. If the iterations diverged or their number exceeded some limiting value (taken to be 20), the integration stepsize was halved, and the computations were repeated from the preceding instant of time.

The convergence of the iterative processes was monitored from the value of the computation error

$$\varepsilon^{(k)} = \max_i \left(\frac{|u_i^{(k)} - u_i^{(k-1)}|}{d_i} \right)$$

where k is the number of the iteration, i is the index of the component of the solution vector, and $d_i = \max(|u_i^{(k)}|, 1)$ is a mixed scaling coefficient. The iterations were broken off when $\varepsilon^{(k)} \le \varepsilon$, where ε is a given admissible error for halting the iterations.

The "Pleiades" problem of celestial mechanics [16]. The motion of seven stars with coordinates $x_i(t)$, $y_i(t)$ and masses $m_i = i (i = 1, \ldots, 7)$ moving in the same plane is described by a system of differential equations

$$\ddot{x}_i = \sum_{j \ne i} m_i \frac{x_j - x_i}{r_{ij}}, \quad \ddot{y}_i = \sum_{j \ne i} m_i \frac{y_j - y_i}{r_{ij}}$$
$$r_{ij} = [(x_i - x_j)^2 + (y_i - y_j)^2]^{3/2}, \quad i, j = 1, \ldots, 7 \tag{5.2}$$

The initial data are

$$\begin{aligned}
&x_1(0) = x_2(0) = 3, \quad x_3(0) = -1, \quad x_4(0) = -3, \quad x_5(0) = -x_6(0) = x_7(0) = 2\\
&y_1(0) = -y_2(0) = 3, \quad y_3(0) = 2, \quad y_4(0) = y_5(0) = 0, \quad y_6(0) = -y_7(0) = -4\\
&\dot{x}_1(0) = \dot{x}_2(0) = \dot{x}_3(0) = \dot{x}_4(0) = \dot{x}_5(0) = 0, \quad \dot{x}_6(0) = 1.75, \quad \dot{x}_7(0) = -1.5\\
&\dot{y}_1(0) = \dot{y}_2(0) = \dot{y}_3(0) = 0, \quad \dot{y}_4(0) = -2.25, \quad \dot{y}_5(0) = 1, \quad \dot{y}_6(0) = \dot{y}_7(0) = 0
\end{aligned} \tag{5.3}$$

The interval of integration with respect to the time parameter t is [0, 3]. The integration stepsize was chosen subject to the condition that the local computation error should not exceed an admissible value of $\delta = 10^{-10}$. The iterations were broken off when $\varepsilon^k \le \varepsilon = 10^{-12}$.

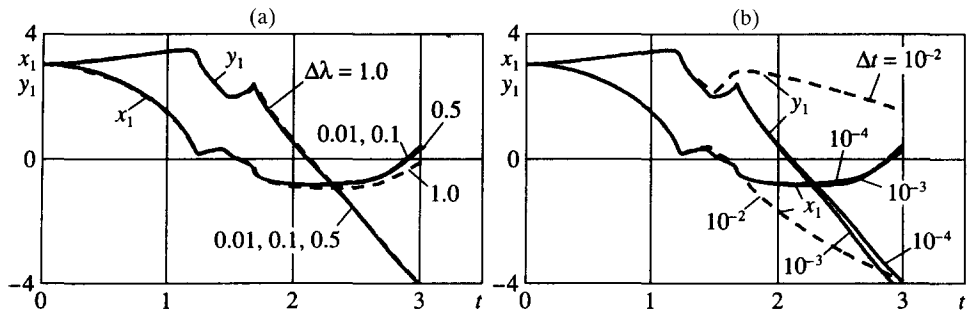

Fig. 1

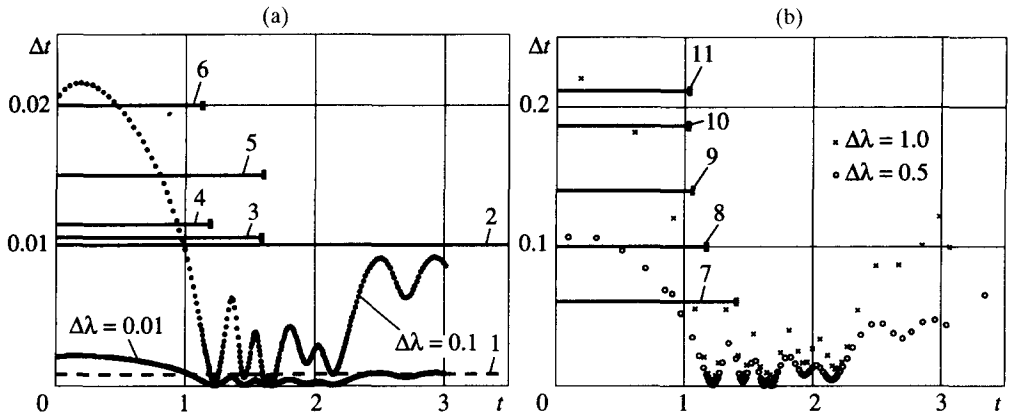

Fig. 2

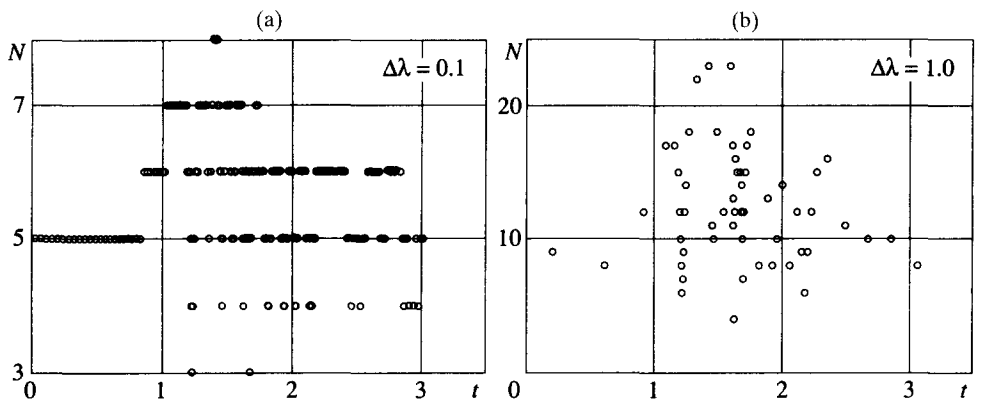

Fig. 3

The results of solving the problem are shown in Figs 1–3. The integration was carried out for several values of the stepsize $\Delta\lambda$ with respect to the parameter of IC length for the parametrized equations and series of values of the stepsize Δt along the given t-interval for the initial problem (5.2), (5.3).

In Fig. 1 we show graphs of the solutions $x_1(t)$, $y_1(t)$ obtained for the parametrized equations for stepsize values $\Delta\lambda = 0.01, 0.1, 0.5$ and 1.0 (a) and those obtained by integrating Eqs (5.2) and (5.3) for stepsize values $\Delta t = 10^{-4}, 10^{-3}$ and 10^{-2} (b). As can be seen, the solution of the parametrized equations varies only slightly when the integration stepsize with respect to IC length is increased substantially (by a factor of 100), while the solution of the equations without parametrization varies considerably when Δt is increased to 10^{-2}. It is also clear that the precision of the integration when $\Delta t > 10^{-3}$ is unacceptable; when $\Delta t > 10^{-2}$ the iterations begin to diverge. When the parametrized equations were integrated, the iterations continued to diverge as $\Delta\lambda$ increased, but the precision of the integration remained unacceptable

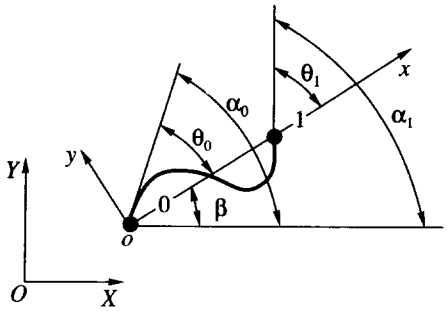

Fig. 4

only when $\Delta\lambda = 1$. An analogous situation was described in [20] for the numerical integration by explicit methods of differential equations with delayed argument.

For every interval $\Delta\lambda$ in step-by-step integration of the parametrized equations, there is a certain corresponding interval Δt, whose length varies as one moves along the IC. Thus, the parametrization automatically adapts the stepsize Δt to the nature of the variation in the IC. This fact is reflected in Fig. 2, where the $\Delta t(t)$ is plotted for values of $\Delta\lambda = 0.01$, 0.1, 0.5 and 1.0, as represented by the dots. Straight-line segments of different lengths correspond to integration of the equations with a constant stepsize without the use of parametrization. The dashed line (labelled *1*) in Fig. 2a represents a certain limiting value of the integration stepsize Δt, which guarantees acceptable precision of the integration. The straight line labelled *2* corresponds to the graphs of the solutions $x_1(t)$, $y_1(t)$ represented by the dashed curves in Fig. 1b for $\Delta t = 10^{-2}$. As indicated above, integration with $\Delta t > 10^{-2}$ leads to diverging iterations. This is shown by the straight-line segments (labelled from *2* to *11*, corresponding to $\Delta t \approx 0.010$, 0.011, 0.012, 0.015, 0.020, 0.060, 0.100, 0.140, 0.180 and 0.220); these segments end at certain values of the time parameter t at which the iterative process begins to diverge.

The dots in Fig. 3 represent the number of iterations as a function of time, when the parametrized equations are integrated with stepsize $\Delta\lambda = 0.1$ and $\Delta\lambda = 1.0$.

Modelling the dynamics of a flexible cantilever rod initially coiled in a ring by a bending moment. We will now consider the problem of the geometrically non-linear dynamic behaviour of an elastic flexible rod attached as a cantilever at one end. In its initial state the rod is coiled into a ring by a bending moment applied at the free end and equal to $2\pi EJ/L$, where EJ is the bending stiffness of the rod and L is its length. At time $t = 0$ the action of the moment is discontinued and a dynamic process (uncoiling) begins in the plane, under the influence of elastic and inertial forces.

The problem is solved in a finite-element setting, using the approach described in [3, 4]. Gravitational forces and damping of the vibrations are not taken into account.

Each element (see Fig. 4) is associated with a local (element) system of coordinates system oxy in such a way that one of the axes (say, ox) passes through the nodes of the element 0.1. Displacements, angles of rotation, linear and rotational velocities of the element axes performing the motion relative to a fixed system of coordinates OXY are rigorously taken into account. The shape functions were taken to be quasi-static approximations of the local displacements and angles of rotation of cross-sections of a rod element in variables of the element system of coordinates. They are constructed by solving an homogeneous linear static problem depending on the angles of rotation of the nodal sections of an element θ_0, θ_1 as functions of time t. The rod is considered to be extensible. It is also assumed that the cross-sections of the elements may be twisted and sheared relative to one another, that is, mean shear deformations are taken into account. To simplify the computations, the distributed mass characteristics of the rod (masses and moments of inertia) and the load are reduced to the nodes of the finite-element model. The generalized coordinates were taken to be the absolute coordinates of the nodes and the angles of rotation of the cross-sections of the rod associated with those nodes relative to the system of coordinates OXY.

The non-linear equations of motion are written in generalized coordinates in the form of Lagrange equations of the second kind

$$m_i\ddot{q}_i + \frac{\partial U^{\Sigma}}{\partial q_i} = Q_i, \quad i = 1, \ldots, N \tag{5.4}$$

where m_i is the ith element of the diagonal matrix of masses, $U^{\Sigma} = U^{(1)} + \ldots + U^{(N)}$ is the potential energy of the system, where $U^{(k)}$ is the potential energy of the kth element, Q_i is the generalized force corresponding to the generalized coordinate q_i with subscript i and N is the number of generalized coordinates. In what follows, to simplify the notation, we will omit superscripts, with the understanding that all the notation refers to the kth element.

The potential energy of an element under finite deformations (taking into account terms quadratic in the angle of rotation of cross-sections) may be written in the form

$$U = \frac{1}{2}\left\{\frac{EJ}{l}[(\alpha_1 - \alpha_0)^2 + 3\kappa(\alpha_1 + \alpha_0 - 2\beta)^2] + \frac{N^2 l}{EF}\right\}$$

The longitudinal force N, which is constant as a function of the length of the element, and the dimensionless coefficient κ are defined as

$$N = EF\left\{\frac{u_1}{l} + \frac{1}{8}\left[\frac{1}{3}(\alpha_1 - \alpha_0)^2 + \frac{\kappa^2}{5}(\alpha_1 + \alpha_0 - 2\beta)^2\right]\right\}, \quad \kappa = \left(1 + \frac{12EJ}{l^2 GF_c}\right)^{-1}$$

The longitudinal displacement of node 1 in the direction of the ox axis relative to node 0 is equal to $u_1 = \sqrt{(X_1 - X_0)^2 + (Y_1 - Y_0)^2} - l$, where l is the length of the element before deformation, β is the angle of rotation of the moving element system of coordinates oxy relative to the inertial system of coordinates OXY, and EJ, EF and GF_c are the bending, tensile-compressive and shear stiffness, respectively.

As a preliminary, a solution was sought to the static problem of the strong deformation of an initially rectilinear rod by a bending moment of the value indicated above. The problem was solved using the best parametrization for the static state equations [15]. The resolvent system of equations in that case has the form

$$\left\| \frac{\partial^2 U^{\Sigma}}{\partial q_i \partial q_j} \right\| \left\| \frac{d}{dp} \right\| \begin{Vmatrix} q_1 \\ \vdots \\ q_N \end{Vmatrix} = \begin{Vmatrix} F_1^* \\ \vdots \\ F_N^* \end{Vmatrix} \tag{5.5}$$

where q_i, F_i^* $(i = 1, \ldots, N)$ are the generalized coordinates and amplitude values of the external nodal forces and moments corresponding to these coordinates. The load parameter p, which was varied within the limits 0 to 1, was related to the argument (the IC length) by the differential relation

$$\frac{dp}{d\lambda} = J^{-1} = \frac{1}{\sqrt{1 + ff}}$$

where f is the vector of the right-hand sides of system (5.5), solved for the derivatives dq_i/dp.

As a result, a configuration was found – a circle of radius $L/(2\pi)$ which defined the initial state of the system for the solution of the dynamic problem.

After parametrization, the system of equations (5.4) becomes

$$v_i' = \frac{1}{Jm_i}\left(Q_i - \frac{\partial U^{\Sigma}}{\partial q_i}\right), \quad q_i' = \frac{v_i}{J}, \quad t' = \frac{1}{J}; \quad J = \sqrt{1 + qq + vv}$$

The vector $q = [q_1, \ldots, q_N]^T$ is the analogue of the vector u in (1.1), $v = [v_1, \ldots, v_N]^T$.

The following parameter values were chosen for the computations: $L = 10$ m, $EF = 2.88 \times 10^7$ N, $EJ = 960$ N m^2 and $GF_c = 1.108 \times 10^7$ N; the mass density was $\rho = 2800$ kg/m^3. The rod was divided into 100 elements of equal length.

The integration was carried out in the interval from 0 to 30 s. The integration stepsize with respect to the length parameter was adapted to the process of constructing the IC on the basis of the estimated local integration error. The maximum admissible local error was taken to be 10^{-9}. Without adaptation of the stepsize to the IC, the integration turned out to be inefficient, requiring large computational resources. The iterations were monitored by estimating the error, with the maximum admissible error taken to be 10^{-10}. Some results of the computations are shown in Figs 5–7.

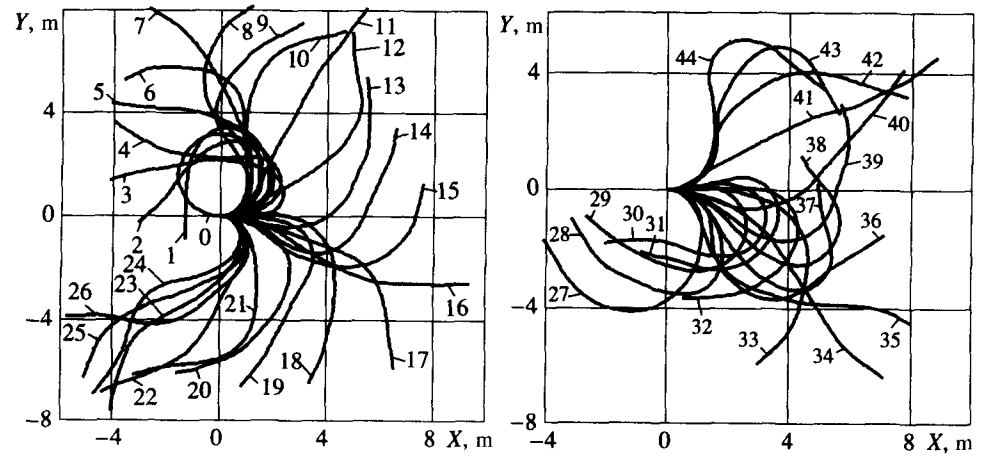

Fig. 5

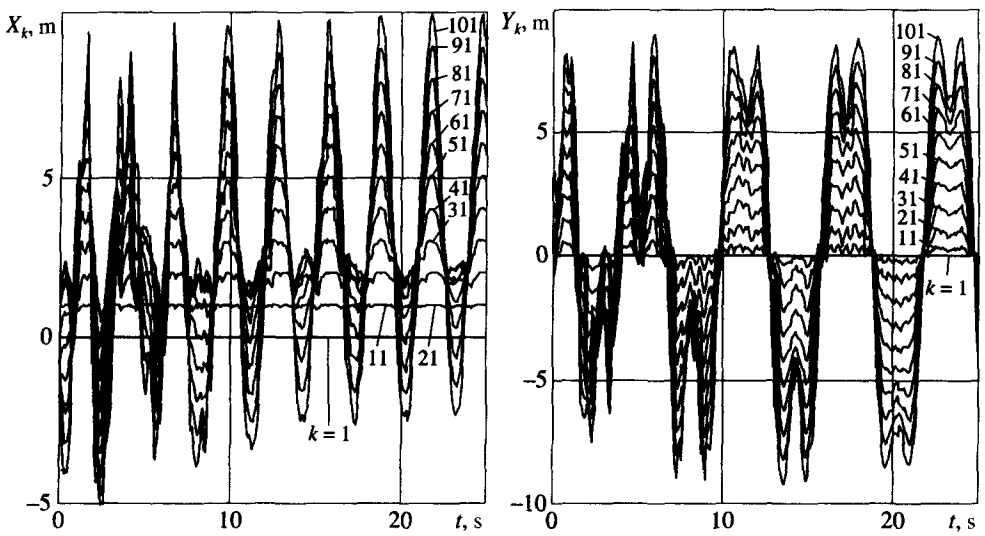

Fig. 6

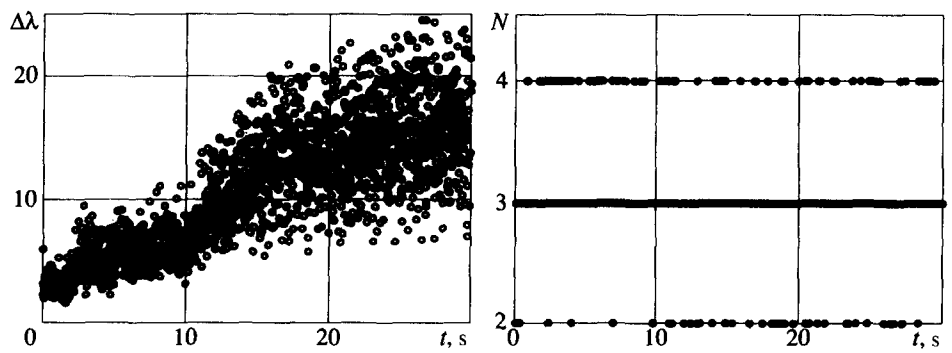

Fig. 7

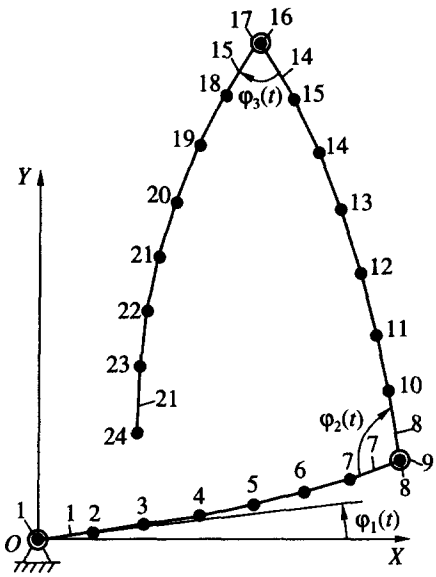

Fig. 8

Figure 5 shows different configurations of the rod corresponding to motion in the interval $0 \le t \le 4.4$ s and arranged in time with a stepsize of about 0.1 s (curves *1–44*). Curve 0 is a circle corresponding to the initial (static) configuration of the rod. Absolute coordinates (in meters) are marked off along the axes of the graphs. Figure 6 plots the nodal coordinates X and Y (measured along the ordinate axis in meters) as functions of the time t (measured along the abscissa axis in seconds). The curves were constructed for several nodes, whose numbers are indicated on the right. The nodes were numbered successively from 1 to 101, beginning with the fixed end and ending with free end. The dots in the left-hand part of Fig. 7 show how the integration stepsize was varied with its adaptation to the construction of the IC based on an estimate of the local computation error; the dots in the right-hand part of the figure represent the number of iterations as a function of time; obviously, with the given parameters of the computational precision, the mean number of iterations was three.

Integration of the equations of motion using algorithm (5.1) with simple iterations, but without the parametrization procedure, proved to be practically impossible: The iterative process diverged at the beginning of the integration for all reasonable values of the integration stepsize.

Integration of the non-parametrized equations based on formulae (5.1) using Newton–Raphson iterations enabled us to solve the problem. This approach, however, turned out to be less effective compared with the method of simple iterations in the parametrized case, because of the complexity of the algorithm being used, which involves computation of the Jacobian and the solution of a linearized system of algebraic equations. The time required to integrate the non-parametrized problem using Newton–Raphson iterations turned out to be about 1.8 times longer than the time required to integrate the parametrized equations using simple iterations; moreover, the difference tended to increase markedly as the dimensionality of the problem (the number of finite elements) was increased. Integration of the problem using a modified Newton–Raphson method also yielded no advantage, needing about 1.5 times more time than integration of the parametrized equations.

Modelling the dynamics of the unfolding of a system consisting of three flexible rods coupled by hinges. Consider a system of three flexible rods joined together in succession by hinges. It is assumed that the cross-sections of the rods have the same geometric and stiffness characteristics. The following parameter values were chosen for the calculations: $EF = 7.2 \times 10^6$ N, $EJ = 60\ N\ m^2$, $GF_c = 2.7692 \times 10^6$ N, and mass density $\rho = 2800$ kg/m^3.

The problem is solved in a finite-element setting, analogous to that used in the preceding problem of an uncoiling cantilever rod. Gravitational forces and damping of the vibrations are not taken into account.

A finite-element model of the system is illustrated in Fig. 8, which illustrates the enumeration of the finite elements and nodes (the numbers of the finite elements from 2 to 6, from 9 to 13 and from 16 to 20 are omitted). Node 1 is assumed to be stationary in space ($x_1 = y_1 = 0$), but it may rotate freely relative to the system of coordinates OXY. Each rod is of length $L = 2$m. The model consists of 21

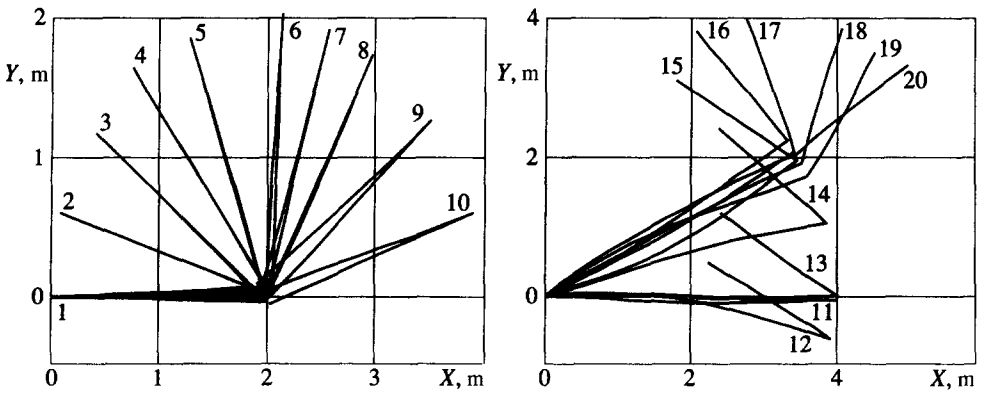

Fig. 9

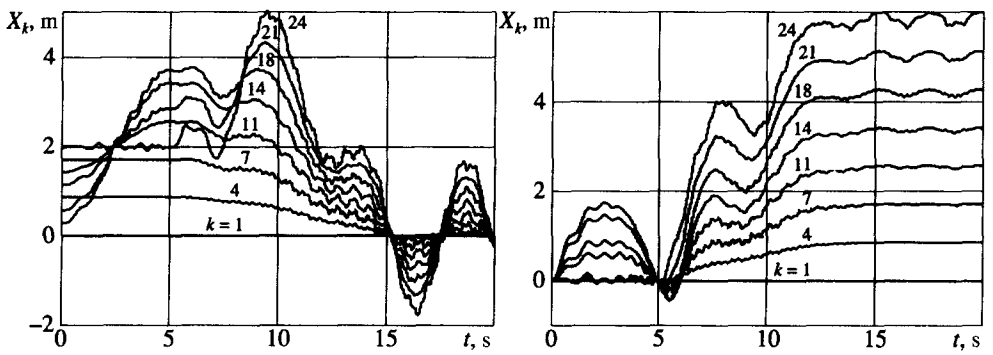

Fig. 10

finite elements and 24 nodes. All the finite elements of the system are identical and of length $l = 0.2857$ m. Nodes 8, 9 and 16, 17 from the hinges, which may be displaced without restriction. The initial configuration of the system is a straight horizontal line of length $L = 2$ m. This is the state corresponding, e.g. to a "packaging" of the system in which the angle between element 1 and the OX axis is $\varphi_1(0) = 0$, the angle between elements 7 and 8 is $\varphi_2(0) = \pi$, and the angle between elements 14 and 15 is $\varphi_3 = 0$.

The system is "unfolded" by changing the angles, in a prescribed manner, between the axes of the rods where they are hinged together, and by similarly changing the angle between the axis of the rod hinged at node 1 and the direction of the OX axis. First the angle $\varphi_2(t)$ is opened out in the clockwise direction, then the angle $\varphi_3(t)$ in the clockwise direction, and the angle $\varphi_1(t)$ in the counterclockwise direction, as given functions of time, where t is the time in seconds. The law governing the "unfolding" of the system is defined by the formulae

$$\varphi_1(0 \le t \le 5) = 0, \quad \varphi_1(5 \le t \le 15) = \frac{t-5}{10}\frac{\pi}{2}, \quad \varphi_1(t > 15) = \frac{\pi}{2}$$

$$\varphi_2(0 \le t \le 5) = -\frac{t}{5}\pi, \quad \varphi_2(t > 5) = -\pi$$

$$\varphi_3(0 \le t \le 5) = 0, \quad \varphi_3(5 \le t \le 10) = -\frac{t-5}{5}\pi, \quad \varphi_3(t > 10) = -\pi$$

The integration was carried out for motion of the system in the time range from 0 to 20 s. The integration stepsize with respect to the continuation parameter was adapted to the IC construction process on the basis of the estimated local computation error. The maximum admissible local error was taken to be 10^{-8}. The iterations, in turn, were monitored by estimating the computation error, whose maximum admissible value was taken to be 10^{-10}. The results of the integration are shown in Figs 9–11.

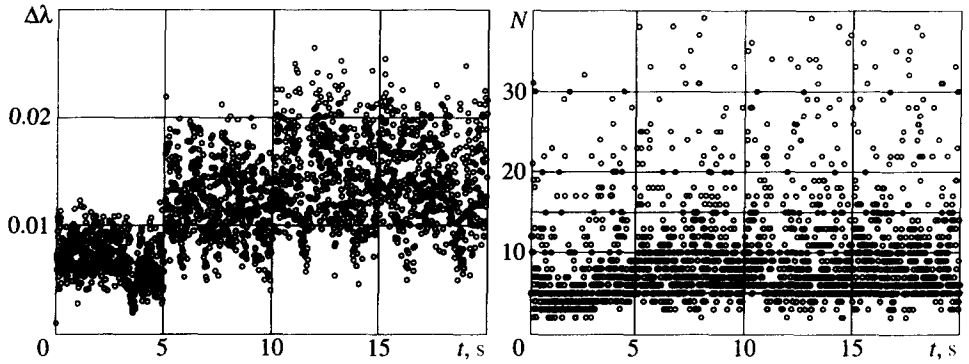

Fig. 11

In Fig. 9 we show various configurations of the rod system corresponding to motion in the interval $0 \le t \le 10$ s and arranged in time with a stepsize of around 0.5 s (curves *1–20*). Figure 10 plots the coordinates X_k, Y_k as functions of the time t for a selected series of node numbers t. The dots in the left-hand part of Fig. 11 represent the changes in the integration stepsize as it adapts to the process of IC construction based on the estimated local computation error; the dots in the right-hand part represent the dependence of the number of iterations on the time. For the specified values of the precision parameters, the mean number of iterations is 7–8.

Computations without adapting the stepsize to the IC (based on the estimated local integration error) proved to be extremely ineffective. Integration of the equations of motion of the structure under consideration using algorithm (5.1), without using the parametrization procedure, is practically impossible, since simple iterations diverge at the very start of the integration for all reasonable values of the integration stepsize.

As in the previous problem, integration of the non-parametrized equations using Newton–Raphson iterations or a modified version thereof enabled the problem to be solved. However, this was less effective compared with the procedure of integrating the parametrized equations using simple iterations. The time required turned out to be about 1.6 times longer for Newton–Raphson iterations and 1.4 times longer for modified Newton–Raphson iterations. Moreover, the difference between the computing times increased as the dimensionality of the problem increased.

This research was supported financially by the Russian Foundation for Basic Research (03-01-000-71, 01-01-00038).

REFERENCES

1. LUR'YE, A. I., *Analytical Mechanics*. Fizmatgiz, Moscow, 1961.
2. BATHE, K.-J. and WILSON, E. L., *Numerical Methods in Finite Element Analysis*. Prentice-Hall, Englewood Cliffs, NJ, 1976.
3. DANILIN, A. N., Non-linear equations of motion of flexible rod systems. *Izv. Ross. Akad. Nauk. MTT*, 1994, 1, 177–188.
4. DANILIN, A. N., Two-dimensional problem of the dynamics of space systems with flexible one-dimensional elements. *Vestnik MAI*, 1995, **2**, 2, 61–68.
5. SHKLYARCHUK, F. N., Non-linear and linearized equations of motion of elastic space structures. *Izv. Ross. Akad. Nauk. MTT*, 1996, 1, 161–175.
6. DANILIN, A. N., GRISHANINA, T. V., SHKLYARCHUK, F. N. and BUZLAEV, D. V., Dynamics of a space vehicle with elastic deploying tether. *Comput. and Structures*, 1999, **72**, 1–3, 141–147.
7. PONTRYAGIN, L. S., *Ordinary Differential Equations*. Nauka, Moscow, 1982.
8. ARNOL'D, V. I., *Ordinary Differential Equations*. Nauka, Moscow, 1984.
9. GRIGOLYUK, E. I. and SHALASHILIN, V. I., *Problems of Non-linear Deformation*. Nauka, Moscow, 1988.
10. SHALASHILIN, V. I. and KUZNETSOV, Ye. B., The Cauchy problem for non-linearly deformable systems as a problem of parametric continuation of the solution. *Dokl. Ross. Akad. Nauk*, 1993, **329**, 4, 426–428.
11. KUZNETSOV, Ye. B. and SHALASHILIN, V. I., The Cauchy problem as a problem of parametric continuation of the solution. *Zh. Vychisl. Mat. Mat. Fiz.*, 1993, **33** , 12, 1792–1805.
12. SHALASHILIN, V. I. and KUZNETSOV, Ye. B., The best parameter of continuation of the solution. *Dokl. Ross. Akad. Nauk*, 1994, **334**, 5, 566–568.
13. KUZNETSOV, Ye. B. and SHALASHILIN, V. I., The Cauchy problem for mechanical systems with a finite number of degrees of freedom as a problem of continuation with respect to the best parameter. *Prikl. Mat. Mekh.*, 1994, **58**, 6, 14–21.
14. SHALASHILIN, V. I. and KUZNETSOV, Ye. B., *The Method of Parametric Continuation and Best Parametrization*. Editorial URSS, Moscow, 1999.

15. DANILIN, A. N. and SHALASHILIN, V. I., The parametrization of the non-linear equations of deformation of a rigid body. *Izv. Ross. Akad. Nauk. MTT*, 2000, 1, 82–92.
16. HAIRER, E., NORSETT, S. P. and WANNER, G., *Solving Ordinary Differential Equations. Nonstiff Problems*. Springer, Berlin, 1987.
17. HAIRER, E. and WANNER, G., *Solving Ordinary Differential Equations. Stiff and Differential-Algebraic Problems*. Springer, Berlin, 1996.
18. BAKHVALOV, N. S., *Numerical Methods*, Vol. 1. Nauka, Moscow, 1973.
19. DANILIN, A. N., KUZNETSOV, E. B. and SHALASHILIN, V. I., The best parametrization and numerical solution of the Cauchy problem for a system of ordinary differential equations of second order. *Functional Differential Equations*, 2001, **8**, 1–2, 141–146.
20. KOPYLOV, A. V. and KUZNETSOV, Ye. B., An approach to the numerical integration of the Cauchy problem for a differential equation with delay. *Zh. Vychisl. Mat. Mat. Fiz.*, 2001, **41**, 10, 1547–1556.

Translated by D.L.